Genetically Driven CD39 Expression Affects Sezary Cell Viability and IL-2 Production and Detects Two Patient Subsets with Distinct Prognosis

JID Open

Mario Picozza[1,4], Cristina Cristofoletti[2,4], Antonella Bresin[2], Martina Fioretti[2], Manolo Sambucci[1], Enrico Scala[2], Alessandro Monopoli[2], Maria Cantonetti[3], Maria Antonietta Pilla[2], Maria Pina Accetturi[2], Giovanna Borsellino[1], Stefania D'Atri[2], Elisabetta Caprini[2], Giandomenico Russo[2] and Maria Grazia Narducci[2]

Sézary syndrome (SS) is a rare and aggressive variant of cutaneous T-cell lymphoma. It is characterized by the copresence of CD4+ neoplastic lymphocytes, named Sezary cells, mainly in the blood, lymph nodes, and skin where they induce chronic inflammation that in turn impairs the patient's QOL and fuels neoplastic cells. SS is not readily cured, but immunotherapy is becoming an effective option for this lymphoma. In this study, we investigated, in a large cohort of patients with SS, the expression and function of the immune checkpoint molecule CD39, which degrades proinflammatory extracellular adenosine triphosphate. We showed that the SNP rs10748643 A/G within the *ENTPD1* gene coding for the CD39 protein controls its expression level. Patients carrying the A/G−G/G genotype showed a significantly higher frequency of clonal CD4+CD39+ SS cells than those carrying the A/A genotype. Different from other cancers, high CD39 expression correlates with a better prognosis. Comparing primary G/G with A/A lymphoma cells, we observed that G/G SS cells have a higher ability to degrade adenosine triphosphate, increased apoptotic susceptibility, and upon activation, reduced IL-2 production. Accordingly, CD39 enzymatic inhibition enhances SS cell viability and IL-2 production on activation. These results strongly suggest a special caution for SS treatment with therapeutic inhibitors of CD39.

Journal of Investigative Dermatology (2022) **142,** 3009−3019; doi:10.1016/j.jid.2022.04.017

INTRODUCTION

Sézary syndrome (SS) is a rare aggressive leukemic variant of cutaneous T-cell lymphoma in which the CD4+ neoplastic lymphocytes, named Sezary cells, accumulate in the blood, lymph nodes, and skin causing chronic inflammation (Scarisbrick et al., 2015; Willemze et al., 2005).

No specific therapy is available yet to treat SS (Wilcox, 2017); however, immunotherapies such as extracorporeal photopheresis (Gao et al., 2019; Ling et al., 2020) and allogeneic bone marrow transplantation (Shalabi et al., 2019) are associated with prolonged and durable remissions. Recently, immune checkpoint inhibitors, including anti−PD-1 and anti-CTLA4 mAbs have been employed with some success in cutaneous T-cell lymphoma (Gibson et al., 2013; Khodadoust et al., 2020; Narducci et al., 2020), but it is still necessary to investigate on immune checkpoint receptors to improve the therapeutic responses.

In this study, using polychromatic flow cytometry (FC), we found that CD49d downregulation together with CD39 expression, two markers already independently described in SS cells (Bensussan et al., 2019; Scala et al., 2010), well discriminate SS cells from the healthy T-cell counterpart. Regulatory T cells are CD49d− CD39+, and we and others previously proved that CD39 expression is mainly associated with the immune-suppressive activity of these cells (Borsellino et al., 2007; Deaglio et al., 2007). Indeed, CD39 degrades the proinflammatory extracellular adenosine triphosphate (ATP) and contributes, together with CD73, to generate immunosuppressive extracellular adenosine in the tumor microenvironment (Moesta et al., 2020).

CD39 expression is genetically controlled by the SNP rs10748643 A/G within the promoter region of its coding gene *ENTPD1* (Friedman et al., 2009), as shown in regulatory T cells (Rissiek et al., 2015), peripheral activated CD4+ T cells (Fang et al., 2016), and tumor-infiltrating CD8+ T cells (Gallerano et al., 2020).

In this study, we investigated the relationship between SNP rs10748643 and CD39 expression, the impact of CD39 expression on patient survival, the enzymatic activity of CD39, and its autocrine roles in primary lymphoma cells.

[1]*Neuroimmunology Lab, IRCCS Fondazione Santa Lucia, Rome, Italy;* [2]*Istituto Dermopatico dell'Immacolata, Istituto di Ricovero e Cura a Carattere Scientifico, Rome, Italy; and* [3]*Department of Hematology, University of Tor Vergata, Rome, Italy*

[4]*These authors contributed equally to this work.*

Correspondence: Maria Grazia Narducci, *Istituto Dermopatico dell'Immacolata, Istituto di Ricovero e Cura a Carattere Scientifico, Via dei Monti di Creta 104, Rome 00167, Italy. E-mail: narducci@idi.it; m.narducci@idi.it*

Abbreviations: ATP, adenosine triphosphate; FC, flow cytometry; HD, healthy donor; SS, Sézary syndrome

Received 1 August 2021; revised 29 March 2022; accepted 14 April 2022; accepted manuscript published online 6 May 2022; corrected proof published online 26 August 2022

RESULTS

A 13-color FC analysis refines the immunophenotype of SS cells

Polychromatic FC was employed to profile the surface markers of SS cells using an antibody panel that included CD3, CD4, CD25, CD39, CD49d, CCR7, CD62L, CD127, CD158k (KIR3DL2), and PD-1. CD8 and CD19 antibodies, together with a live/dead discrimination dye, were also used to accurately gate out unwanted cells, whereas PD-1, CD158k, and CD39 markers were included for their potential therapeutic impact on cutaneous T-cell lymphoma (Bagot et al., 2019; Khodadoust et al., 2020; Narducci et al., 2020; Perrot et al., 2019). PBMCs obtained from three healthy donors (HDs) and five patients with SS, including one with one follow-up sample, were stained and analyzed by Uniform Manifold Approximation and Projection analysis (Becht et al., 2019), which revealed a clear segregation between the majority of cells coming from either HDs or patients with SS (red and blue contours, respectively, in Figure 1a).

The distribution of surface markers was then visualized on the Uniform Manifold Approximation and Projection. CD127+, CD25+, CD62L+, and CCR7+ cells were scattered among the plot areas of both HD and SS cells, indicating a highly variable pattern of expression and a poor discriminative potential between malignant and healthy T cells (Figure 1b). In contrast, CD39+, CD158k+, and PD-1+ cells formed discrete clusters on the SS portions of the map, and CD49d+ cells mapped the HD plot area, suggesting selectivity for either SS and HD cells (Figure 1b). Conventional bivariate plotting of CD49d, CD39, CD158k, and PD-1 markers clearly showed the dichotomy between SS cells and the respective healthy T-cell counterpart. As shown, all patients' aberrant cells were PD-1 positive and CD49d negative or weakly positive; in four of five patients, SS cells were further CD39 positive, whereas they showed an evident expression of CD158k only in two patients (Figure 1c).

The frequency of CD39+CD4+ cells identifies two distinct groups of patients with SS

PD-1 and CD158k expression by SS cells have been largely described (Poszepczynska-Guigné et al., 2004; Samimi et al., 2010). We therefore focused on CD39 and CD49d. Using FC, we stained PBMCs obtained from a new cohort of 11 HDs and from additional 20 patients with SS (whose clonal parameters are shown in Table 1) to investigate the expression pattern of CD39 and CD49d on circulating CD4+ lymphocytes as shown in Figure 2a.

As aspected, we observed a significantly lower frequency of CD49d-positive cells among CD4+ lymphocytes in 19 of 20 (95%) patients (mean value = 15.47 ± 4.6) than among HDs (mean value = 61.33 ± 5; $P \leq 0.0001$), confirming our previous findings (Scala et al., 2010) (Figure 2b and Table 1).

In contrast, we found a clear bimodal distribution in the percentage of CD39+ cells that distinguished the two groups of patients with SS: one group referred to as $CD39^{low}$ with a low percentage of CD39+CD4+ cells (n = 12, mean of frequency values = 4.6 ± 1.3%), comparable with that observed in HDs (n = 11, mean of frequency values = 4.63 ± 2.33%), and one group referred to as $CD39^{high}$ characterized by a high percentage of CD39+CD4+ cells (n = 13, mean of frequency values = 76.6 ± 5.7%) (Figure 2c and Table 1).

Next, we wondered whether both CD4+CD39− and CD4+CD39+ cells respectively found in $CD39^{low}$ and $CD39^{high}$ patients were neoplastic cells. With this aim, we stained PBMCs with specific anti−TCR-Vβ mAbs representing the simplest and the most direct tool for detection of SS clonality (Scala et al., 2002) in combination with anti-CD3, anti-CD4, and anti-CD39 antibodies in 5 of 25 patients with SS. The results confirmed that gated CD4+CD39−cells (Figure 2d) and CD4+CD39+ cells (Figure 2e) largely coincided with clonal cells (Table 1).

CD39 expression in circulating SS cells is genetically defined and has a prognostic relevance for patients with SS

SNP rs10748643 A/G within the promoter region of the *ENTPD1* gene coding for CD39 protein regulates its expression level in regulatory T cells (Rissiek et al., 2015), normal CD4+ T cells (Fang et al., 2016), and tumor-infiltrating CD8+ T cells (Gallerano et al., 2020) but neither in monocytes nor in B cells (Melchiotti et al., 2014). We analyzed the nucleotide sequence of SNP rs10748643 in 24 of the 25 patients with SS evaluated for CD39 expression by FC. Sequencing analysis revealed that individuals with homozygous G/G or heterozygous A/G SNP were endowed with a significantly higher frequency of CD39+CD4+ cells (n = 12, mean value = 76.7 ± 5.8) than patients with homozygous A/A SNP (n = 12, mean value 5.8 ± 1.3; $P \leq 0.0001$) (Figure 3a and b and Supplementary Table S1). These results indicate that *ENTPD1* SNP genotype controls the expression of CD39 also in SS cells.

Next, we evaluated whether the rs10748643 genotype, inferred by a previous SNP6 array study conducted in a cohort of 47 patients, including the 25 individuals analyzed in this study (Cristofoletti et al., 2019, 2013) (Supplementary Table S1), showed any correlation with patient overall survivals in a retrospective analysis.

Kaplan−Meier estimator revealed that A/G and G/G patients have a better prognosis (median of survival of 67 months) than A/A patients (median of survival of 42.6 months) ($P = 0.015$) (Figure 3c). Given that the *ENTPD1* gene maps at chromosome 10q24.1, a locus close to the *PTEN* gene frequently lost in SS and associated with the worst prognosis (Cristofoletti et al., 2019, 2013), we also performed a Kaplan−Meier analysis excluding patients harboring *PTEN* deletion. Even using this stringent rule, the A/G and G/G genotypes continued to be associated with a better prognosis than the A/A genotype (median of survival of A/G and G/G patients = 79 months vs. median of survival of A/A patients = 59 months, $P = 0.05$) (Supplementary Figure S1 and Supplementary Table S1), indicating that independently from the PTEN genomic status, CD39 expression has a favorable impact on SS prognosis.

ENTPD1 genotype controls CD39 expression and persistence on anti-CD3/CD28 activation and its enzymatic activity in untreated SS cells

We next wondered whether *ENTPD1* genotype could control CD39 expression not only in the basal conditions but also upon cell activation. For this purpose, we monitored CD39 expression in PBMCs obtained from G/G (n = 3) and A/A (n =

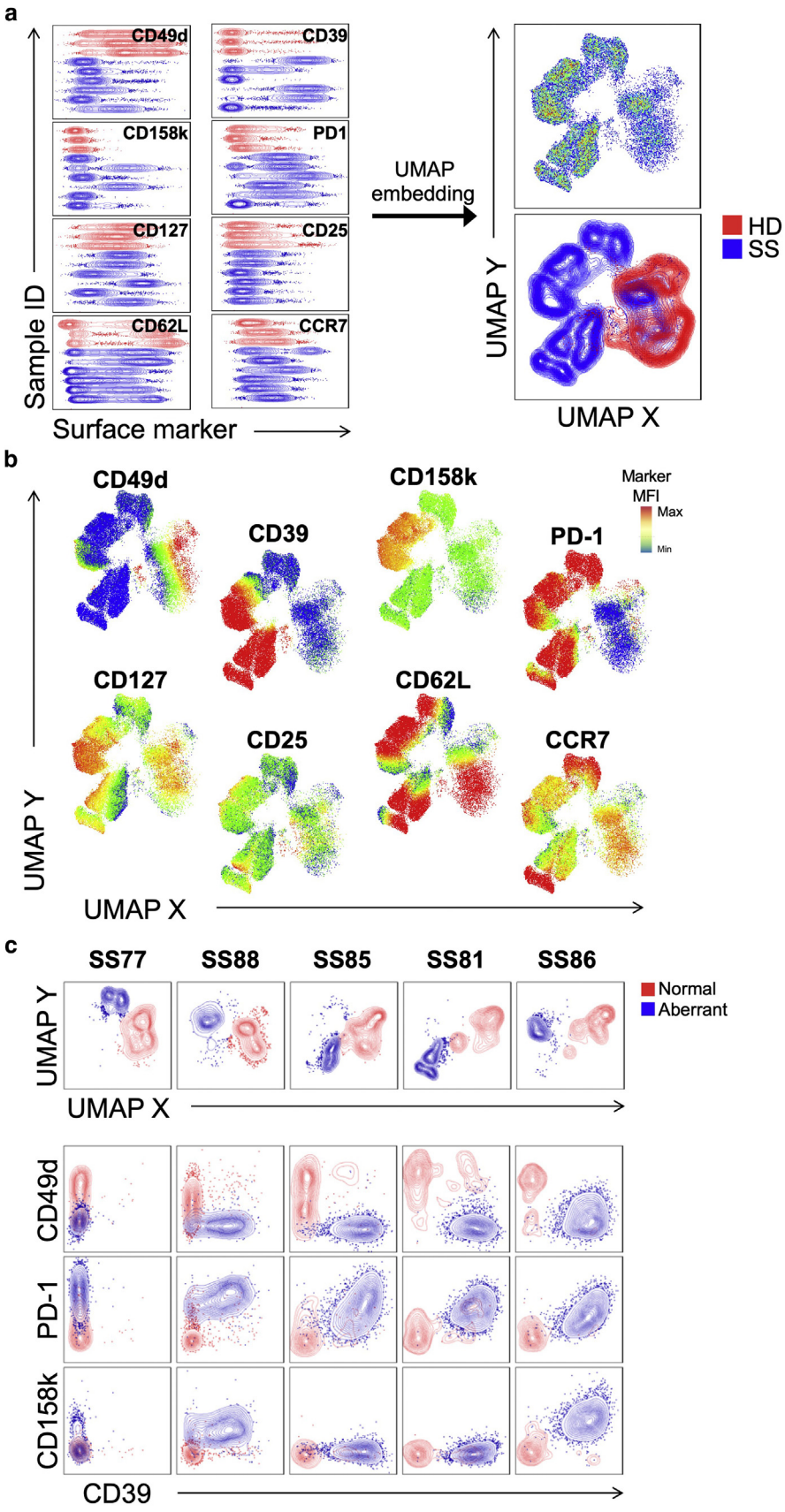

Figure 1. Dimensional reduction analysis unravels defining markers and phenotypic heterogeneity in SS CD4+ T cells. **(a)** Gated CD4+ T cells color coded by health status (five patients with SS + one F-up [blue] vs. three HD [red]) are visualized separated on the y-axis by respective sample IDs and along the eight indicated surface markers, which were submitted to derive UMAP embedding (left panels). **(b)** The distribution of the eight phenotypic markers on the UMAP axes is conveyed by colors according to FIs. **(c)** Separate contour plots showing the distribution on UMAP projections and on CD49d, CD158k, PD-1, and CD39 axes for each of the five patients with SS analyzed (cells from patient SS88 are shown only for T2). Aberrant (blue) and HD-like (red) cells are superimposed in each plot. FI, fluorescence intensity; F-up, follow-up; HD, healthy control; ID, identity; Max, maximum; MFI, median of fluorescent intensity; Min, minimum; SS, Sézary syndrome; T2, day 2; UMAP, Uniform Manifold Approximation and Projection.

Table 1. Clinical Features of Patients Analyzed for CD39 and CD49d Expression

SS ID	Age/ Sex	Time from Diagnosis (mo)	Therapy	TCR-Vβ Family	% TCR-Vβ+ within CD3+/CD4+	% of CD39+SS Cells within Total CD3+/CD4+	% of CD49d+SS Cells within Total CD3+/CD4+
30[1]	52/F	105	89 ECP + IFN-α + s. ster.	13.1	97	76.4	1.9
32[2]	80/F	38.5	37 ECP + IFN-α + s. ster.	5.1	85	0.9	13.4
45[2]	80/M	24.5	6 ECP + IFN-α + s. ster.	Null	93	7	1.1
50[2]	64/M	64	Vorinostat	9	71	0.8	11.8
60[1]	77/M	24	24 ECP + IFN-α + s. ster.	Null	91	65.5	17
61[2]	53/M	0	Untreated	23	75	4.7	36.2
64[2]	72/M	38	20 ECP + IFN-α + s. ster.	2	90	14.4	9.5
67[1]	66/F	59	20 ECP + IFN-α + s. ster.	2	82	70.7	89.2
72[1]	66/M	10.1	13 ECP + IFN-α + s. ster.	13.6	25	28.4	34.9
74[2]	69/M	0	Untreated	17	76	6.6	10
76[1]	69/F	23.5	22 ECP + IFN-α + s. ster.	Null	93	88	3.6
77[1]	51/F	9	8 ECP + IFN-α + s. ster.	Null	74	1.1	11
78[2]	82/M	2	2 ECP + IFN-α + s. ster.	Null	95	0.9	12
80[1]	80/M	0	Untreated	Null	53	62.3	7.3
81[1,3]	69/F	0	Untreated	Null	92	81	1.5
82[1]	857F	29.1	28 ECP + IFN-α + s ster	2	95	97	n.d
83[2]	66/M	0	untreated	13.1	76	0.8	12.2
85[1,3]	78/F	29	28 ECP + IFN-α + s ster	13.6	52	94	3.3
86[1,3]	54/F	0	Untreated	Null	97	99.3	7.6
87[1]	61/F	0	Untreated	Null	87	80	n.d
88T2[1,3]	54/M	12	11 ECP + IFN-α + s ster	3	76	56.7	9.9
96[1]	75/M	0	Untreated	13.1	98	99	n.d
98[2]	56/F	0	Untreated	8	60	10	n.d
103[2]	71/M	0	Untreated	5.2	63	3	n.d
105[2]	66/M	0	Untreated	5.1	95	5	n.d

Abbreviations: ECP, extracorporeal photopheresis; F, female; ID, identification; M, male; n.d, not determined; SS, Sézary syndrome; s. ster., systemic steroid.
[1]$CD39^{high}$ patients.
[2]$CD39^{low}$ patients.
[3]Patients analyzed by 13-color flow cytometry.

3) patients (Supplementary Table S2) stimulated with anti-CD3/CD28 beads in complete medium on day 4. Moreover, to measure how persistent the expression of CD39 was, we analyzed the cells 6 days after removing the beads from the cell culture (day 10).

After 4 days of stimulation, G/G SS cells, already displaying an elevated percentage of CD39 positivity at baseline, strongly upregulated CD39 surface density measured as median fluorescence intensity ($P = 0.02$) (Figure 4a and c). A/A SS cells slightly increased the percentage of CD39 positivity and upregulated this protein, although never reaching the levels observed in samples from G/G SS cells ($P = 0.01$) (Figure 4b and c). Similar results were also observed in normal CD4+T cells obtained from healthy G/G and A/A individuals (data not shown) in agreement with a previous study (Fang et al., 2016).

Six days after bead removal (day 10), G/G SS cells maintained the same percentage of CD39+ cells and the level of median fluorescence intensity (Figure 4a and c), whereas A/A SS cells slightly reduced the percentage of CD39 positivity and significantly reduced the median fluorescence intensity ($P = 0.02$) (Figure 4b and c).

In these experiments, activation of SS cells was confirmed by the expression of the activation marker CD25, which was upregulated on day 4 and, differently from CD39, returned to the basal level on day 10 in all samples analyzed (Supplementary Figure S2). These data indicate that *ENTPD1* genotype controls CD39 expression intensity on cell activation and also CD39 persistence possibly acting through a post-translational mechanism.

The strong difference in CD39 expression observed between G/G and A/A genotype prompted us to assess CD39 enzymatic activity. SS cells from G/G (n = 3) and A/A (n = 3) patients (Supplementary Table S2) were incubated with 1 μM ATP, and the supernatants were evaluated for ATP levels at different time points. After 30 minutes, G/G SS cells degraded 80% of ATP, whereas A/A SS cells were unable to degrade ATP (Figure 4d). The CD39 inhibitor ARL67156 blocked ATP degradation by G/G SS cells, whereas it did not alter ATP levels in the culture medium of A/A SS cells (Figure 4d).

Inhibition of CD39 enzymatic activity and low CD39 expression in SS cells enhance cell viability and IL-2 production on anti-CD3/CD28 activation

To evaluate the effects of blocking CD39 enzymatic activity on SS cell viability, we initially used both ARL67156 and POM-1, a CD39 inhibitor previously shown to be more effective than ARL67156 (Wall et al., 2008). As shown in Supplementary Figure S3, we confirmed the higher inhibitory capacity of POM-1 also in our experimental model, and therefore, this inhibitor was used in the subsequent experiments.

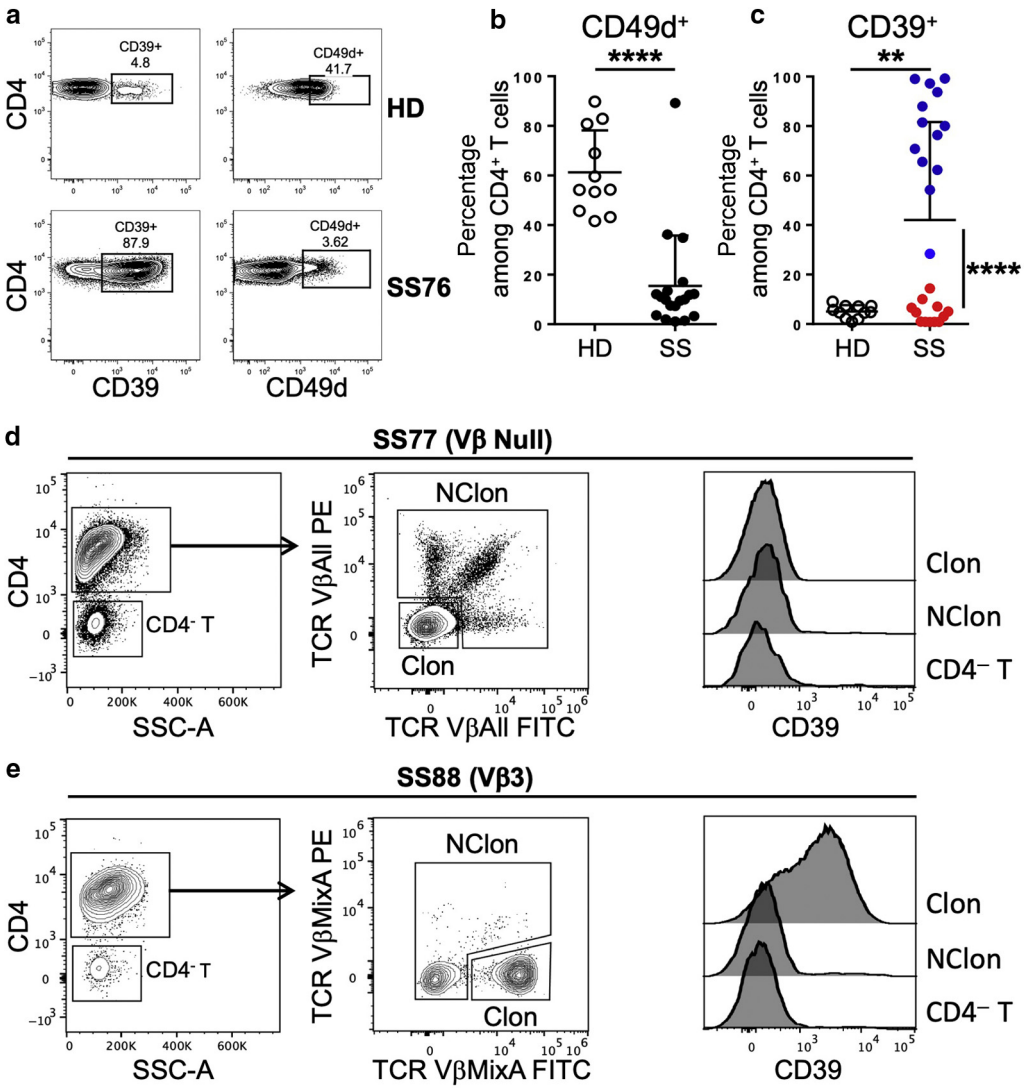

Figure 2. The frequency of circulating CD39+CD4+ identifies two groups of patients with SS. **(a)** CD4+ lymphocytes were analyzed for CD39 and CD49d expression in HDs and patients with SS and representative cases are shown. Numbers inside plots indicate the percentages of positive cells for the indicated antigens. **(b, c)** Percentage of CD4+CD39+ and CD4+CD49d+ cells detected in HDs and patients with SS. Data are expressed as mean ± SD. $^{**}P = 0.004$ and $^{****}P \leq 0.0001$ with two-tails *t*-test. CD39 expression was detected within neoplastic clones recognized by anti-CD3 and anti-CD4 Abs in combination with specific anti−TCR-Vβ Abs confirming that **(d)** CD4+CD39− cells detected in SS77 patient and **(e)** CD4+CD39+ cells detected in patient SS88T2 are Clon. Gated CD8+ T cells (CD4−) and TCR-Vβ−, NClon CD4+ T cells are shown for comparison. Two of the five patients analyzed are shown. Ab, antibody; Clon, clonal; HD, healthy control; Nclon, nonclonal; PE, phycoerythrin; SS, Sézary syndrome; SSC-A, side scatter area.

PBMCs derived from G/G (n = 2) and A/A (n = 4) patients were stimulated for 4 days with anti-CD3/CD28 beads in the absence or presence of 10 μM POM-1 and assayed by FC for cell activation by surface marker expression and for proliferation by CellTrace dilution.

After CD3/CD28 stimulation, we observed a heterogeneous expression level of activation and proliferation markers among all SS samples (Figure 5a). However, as recorded in normal T cells when CD39 is blocked (Li et al., 2019), POM-1 treatment of SS cells significantly increased the percentages of CD25+ ($P = 0.01$), CD71+ ($P = 0.002$), and proliferating ($P = 0.005$) cells in all SS samples, regardless of the genetic status of *ENTPD1* (Figure 5a).

These findings indicate that POM-1 is effective even when SS cells express moderate levels of CD39 as those observed in stimulated A/A SS cells (Figure 4b and c), which under this condition are also able to degrade extracellular ATP, although less effectively than G/G SS cells (Supplementary Figure S4).

Inhibition of CD39 enzymatic activity reduces apoptosis in activated healthy CD4+T cells (Fang et al., 2016). Similarly, POM-1 treatment significantly reduced the frequency of apoptotic activated SS cells derived from all patients (G/G, n = 2; A/A, n = 2) (Figure 5b) ($P = 0.003$) as assessed by staining with Annexin-V.

Taking advantage of patient SS88, which displayed a high degree of variability in CD39 expression on neoplastic cells (Figure 2e and Table 1), we then evaluated apoptosis, without POM-1 usage, in SS cells expressing the highest and the lowest CD39 levels. Patient's PBMC were stimulated with anti-CD3/CD28, and after 6 days, we observed a higher number of apoptotic cells among CD39+SS cells (21.7%, calculated as early 14.6% + late 7.1% apoptotic cells) than

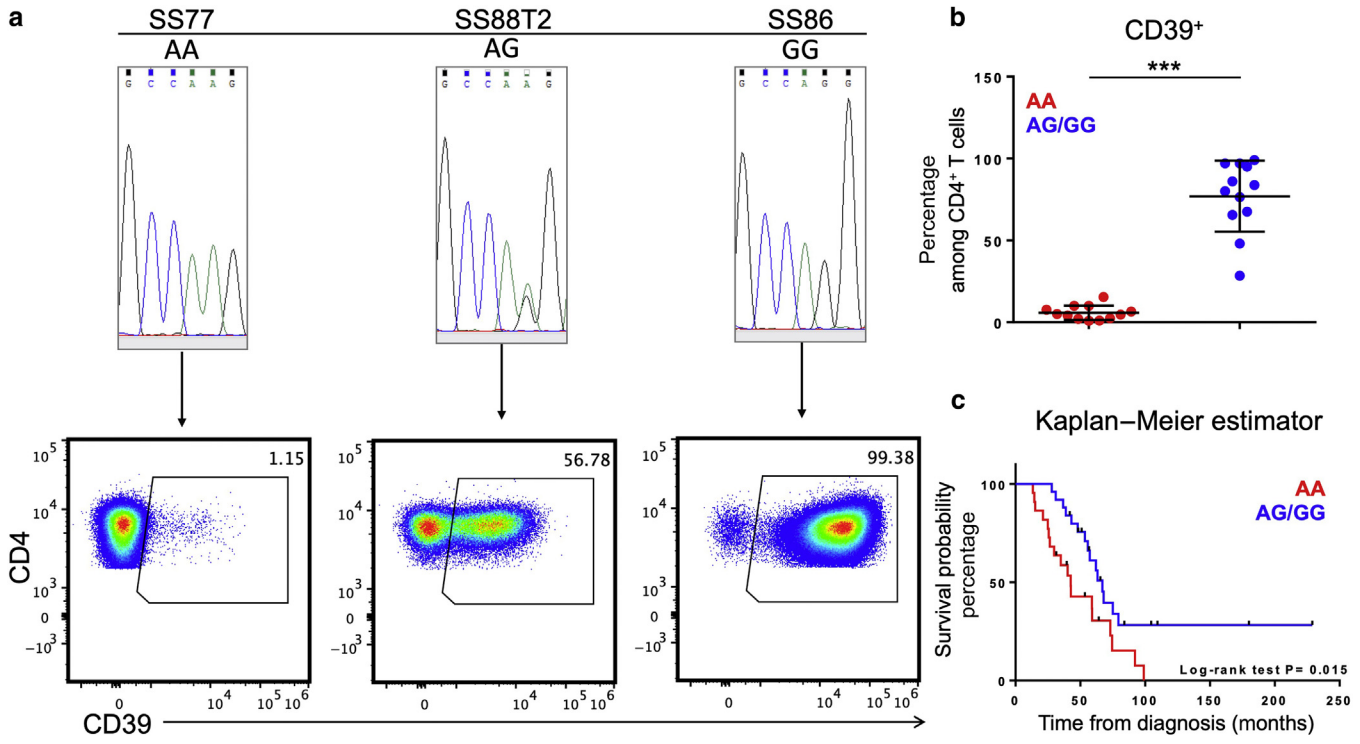

Figure 3. The expression of CD39 in circulating CD4+ T cells is genetically defined and has a prognostic relevance for patients with SS. (a) Representative sequence electropherograms showing the A/A, A/G, and G/G SNP rs10748643 (upper panel) distinguishing patients with SS with a low and high frequency of CD4+CD39+ cells (bottom panel). **(b)** Percentage of CD4+CD39+ cells detected in A/A (n = 12) and A/G and G/G (n = 12) patients with SS. ***$P < 0.0001$ calculated with two-tailed *t*-test. **(c)** Comparison of survival between patients with SS with A/A and AG/GG SNP (n = 47, $P = 0.015$) was calculated by log-rank test. SS, Sézary syndrome.

among CD39- SS cells (14%, calculated as early 8.8% + late 5.2% apoptotic) (Figure 5c). Higher frequencies of apoptotic cells among CD39+ SS cells than among CD39− SS cells were also observed when SS88 PBMCs were cultured in a complete medium alone (Supplementary Figure S5).

CD39 inhibition enhances extracellular ATP level that, in turn, stimulates purinergic receptors, leading to IL-2 production and promoting T-cell effector functions (Li et al., 2019). Because IL-2 promotes SS proliferation through the phosphatidylinositol 3-kinase/protein kinase B/mTOR pathway (Marzec et al., 2008), we evaluated in G/G (n = 2) and A/A (n = 3) samples how POM-1 affected the percentages of IL-2+ SS cells on activation with anti-CD3/CD28 beads and restimulation with phorbol myristate acetate/ionomycin. With the exception of one A/A sample that showed a low percentage of IL-2+ SS cells throughout the experiment, a comparable percentage of IL-2+ SS cells was observed in stimulated G/G and A/A samples (Figure 5d). After POM-1 exposure, a significant increase in the percentage of IL-2+ SS cells in all samples was observed when compared with that in untreated ones (Figure 5d) ($P = 0.03$).

These results prompted us to investigate the functional capacities of G/G and A/A SS cells regarding the IL-2 pathway. For this purpose, we analyzed the expression of *IL2* and *IL2R* at the mRNA level in G/G (n = 7) and A/A (n = 6) SS cells at baseline (day 0) and after 4 days of stimulation with anti-CD3/CD28 beads (day 4) without POM-1 usage. In these experiments, SS cells were not restimulated with phorbol myristate acetate/ionomycin to mimic a more physiological condition. We found low IL-2 expression in all unstimulated samples (Supplementary Figure S6a). On stimulation, A/A SS cells displayed a significantly higher upregulation of *IL2* mRNA than G/G SS cells (Figure 5e and Supplementary Figure S6) ($P = 0.0012$). No significant difference was noted for *IL2R* expression between these two cell subsets (Figure 5e). IL-2 measured by ELISA in supernatants from stimulated G/G (n = 5) and A/A (n = 6) SS cells showed a higher cytokine release in A/A SS cells than in G/G cells (Figure 5f) ($P = 0.015$).

DISCUSSION

Our immunophenotypic analysis of SS cells reveals that concurrent CD49d downregulation and CD39 expression well-characterize SS cells. In this study, we focused on CD39, which degrades the proinflammatory extracellular ATP (Moesta et al., 2020), because it is well-established that skin chronic inflammation feeds SS cells (Krejsgaard et al., 2017).

We found that CD39 expression is genetically controlled by the SNP rs10748643 A/G of the *ENTPD1* (CD39) gene and able to distinguish two groups of patients with SS characterized by a high or low frequency of CD39+ SS cells.

The genetic mechanism that rigorously controls CD39 expression gave us the opportunity to perform a retrospective analysis, correlating the CD39 genotype with survival in 47 patients with SS, including the 25 investigated in this study, which had already been studied by SNP array (Cristofoletti et al., 2019, 2013). We found that $CD39^{high}$ patients carrying the A/G or G/G genotype had a more favorable clinical outcome. These data disagree with previous findings in various human solid cancers (Cai et al., 2016; Mandapathil

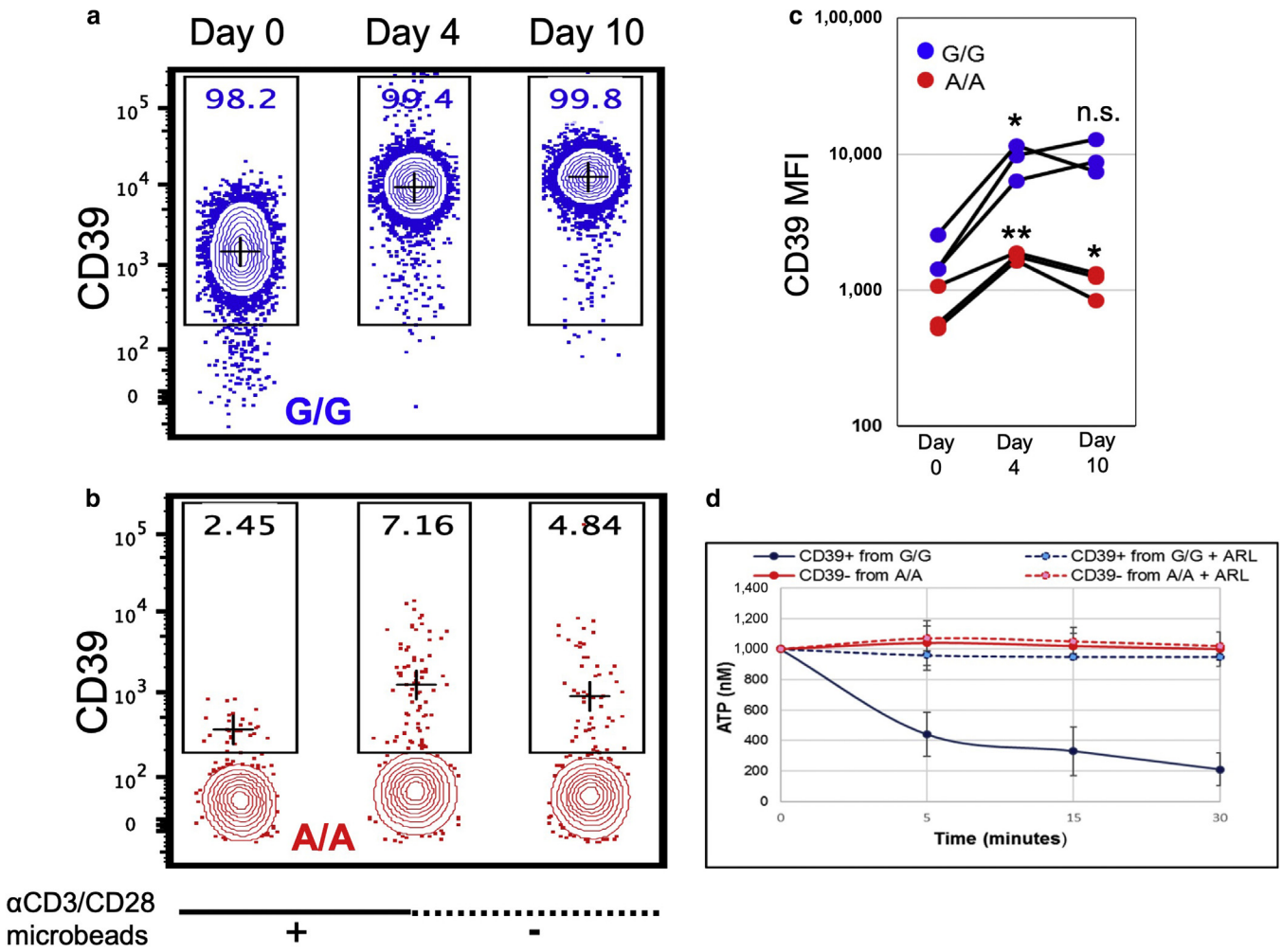

Figure 4. *ENTPD1* genotype controls CD39 expression on cell stimulation and CD39 enzymatic activity in SS cells at baseline. PBMCs from G/G (n = 3) and A/A (n = 3) patients were analyzed by FC on day 0, day 4 after anti-CD3/CD28 stimulation, and 6 days after beads removal (day 10). **(a)** CD39 expression on CD3+CD4+ SS cells in a representative G/G sample (SS96, 98% clonality). **(b)** CD39 expression on CD3+CD4+ SS cells in a representative A/A sample (SS98, 60% clonality). **(c)** Changes in MFI for CD39 expression. **(d)** CD39− SS cells from A/A (n = 3) and CD39+ SS cells from G/G (n = 3) patients were evaluated, at basal conditions, for their ability to degrade ATP with or without ARL67156. Data are presented as mean values (circles) ± SE. $^{**}P = 0.01$ and $^{*}P = 0.02$ with two-tailed paired *t*-test. ATP, adenosine triphosphate; FC, flow cytometry; MFI, median of fluorescent intensity; n.s., not significant; SE, standard error; SS, Sézary syndrome.

et al., 2018; Qi et al., 2020) as well as in hematological diseases such as B-cell chronic lymphocytic leukemia, in which high CD39 expression correlates with a worse prognosis (Pulte et al., 2011). In those tumors, CD39 plays an immunosuppressive role, and because of this effect, several antibodies that specifically antagonize CD39 activity to restore effective immune responses have been recently developed (Perrot et al., 2019). On the contrary, in the T-cell context, CD39 overexpression could take on other meanings as emerges from a study by Fang et al. (2016), in which it was shown that normal activated CD39+ T cells show enhanced apoptotic susceptibility compared with their CD39− T-cells counterpart. These results induced us to investigate in more detail the autocrine rather than paracrine effects of CD39.

Because CD39 blocking has been hypothesized as a therapeutic approach for SS (Bensussan et al., 2019), we first evaluated the effect of CD39 inhibition on SS cell viability. As blood SS cells are mainly in the resting phase, we conducted these experiments under polyclonal stimulation to mimic skin-derived SS cells, which are activated, proliferate, and survive, thanks to signals released by the skin-tumor microenvironment (Cristofoletti et al., 2019; Herrera et al., 2021). We observed that POM-1 treatment enhanced the expression of activation/proliferation markers and reduced apoptosis in SS cells derived from both G/G and A/A patients. We also measured the frequency of apoptotic CD39+ and CD39− SS cells concurrently obtained from patient SS88, and we found that CD39+ SS cells displayed a susceptibility to apoptosis greater than that of the CD39− counterpart both after stimulation and under basal conditions.

CD39 inhibition induces T helper 1 cytokine production (Li et al., 2019). Among them, we focused on IL-2, a GF for cutaneous T-cell lymphoma cell lines (Döbbeling et al., 1998), primary SS cells (Foss et al., 1994), and activated normal T cells in which it promotes expansion through IL-2R (CD25) binding (Spolski et al., 2018).

We observed that POM-1 treatment enhanced the percentage of IL-2+ SS cells in all the activated samples analyzed. Deepening this topic, we also found that A/A SS cells showed a significantly increased functionality on anti-

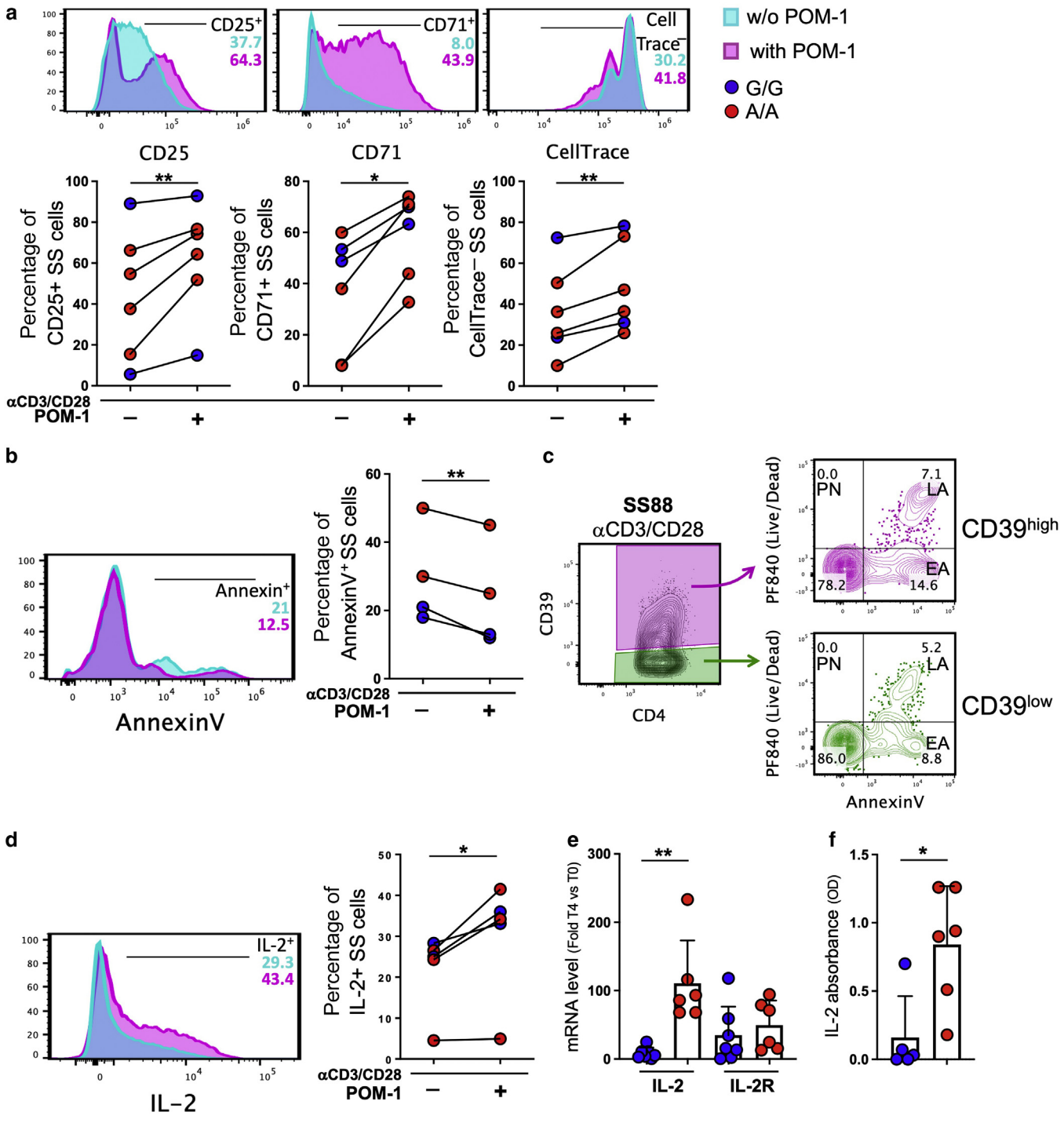

Figure 5. Inhibition of CD39 enzymatic activity and low CD39 expression in SS cells enhances cell viability and IL-2 production on anti-CD3/CD28 activation. (a) Top: representative CD25, CD71, and CellTrace staining in SS cells stimulated by anti-CD3/CD28 beads without or with POM-1. Bottom: summary graphs showing the percentages of CD71+, CD25+, and CellTrace− SS cells (n = 6). **(b)** Representative annexin-V SS cells staining and statistic (n = 4). **(c)** EA and LA cells in gated CD39^{high} and CD39^{low} SS cells from patient SS88 after 6 days of activation. No PN SS cells were detectable. **(d)** Representative intracellular IL-2 staining in SS cells and statistic (n = 5). **(e)** qRT-PCR for IL-2 and IL-2R. **(f)** ELISA for the IL-2 released on stimulation. $^{**}P \leq 0.003$ and $^{*}P \leq 0.03$ with (**a**–**d**) paired or (**e, f**) unpaired two-tailed *t*-test. EA, early apoptotic; LA, late apoptotic; OD, optical density; PN, primary necrotic; SS, Sézary syndrome; w/o, without.

CD3/CD28 stimulation because they produced higher IL-2 levels than G/G SS cells, whereas a similar IL-2R expression level was observed in both SS subsets. These data seem to suggest a proliferative advantage of A/A SS cells through the IL-2/IL-2R binding, which activates, among others, the phosphatidylinositol 3-kinase/protein kinase B/mTOR pathway that is frequently deregulated at the genetic level and hyperactivated in SS (Cristofoletti et al., 2019; Marzec et al., 2008; Mirza et al., 2020)

Because CD39 is a key marker for suppressor activity of regulatory T cells (Borsellino et al., 2007; Deaglio et al., 2007), we must necessarily consider that SS cells from A/G and G/G patients, potentially releasing more extracellular adenosine compared with A/A SS cells, could weaken the

host's immune response, enacting another immune escape mechanism, as recently shown in CD39+ acute T-cell leukemia (Nagate et al., 2021). This hypothesis is reinforced by the lack of CD26 on the SS cell surface (Narducci et al., 2006; Olsen et al., 2011), an enzyme that, linked to adenosine deaminase, reduces local extracellular adenosine concentration by converting it into inosine (Cortés et al., 2015). This immunosuppressive mechanism that impairs normal T-cell function can curb the proliferation of SS cells, as recently observed (Sonigo et al., 2022). This last scenario, combined with a greater fragility observed in CD39+ SS cells, could represent a benefit for A/G−G/G patients and explain the better prognosis observed in this subset of patients with SS.

This study describes a previously unreported inherited genetic marker able to distinguish two subtypes of patients with SS. One limitation of our study is the small number of patients studied in functional experiments. Thus, also considering the high interindividual and intratumoral heterogeneity recently documented in SS (Herrera et al., 2021; Park et al., 2021; Rassek and Iżykowska, 2020), further studies need to be done on a larger number of SS samples to understand how CD39 expression influences the different functional behavior observed in CD39+ and CD39− SS cells and to intercept potentially targetable pathways in this lymphoma. Indeed, despite CD39 antagonists emerging as therapeutics for many tumors (Perrot et al., 2019), special caution should be made for SS because CD39 inhibition, as shown in our cohort of patients with SS, accelerates the proliferation rate and promotes IL-2 production and resistance to apoptosis in the malignant cells and could sustain the chronic skin inflammation associated with tumor progression and poor QOL.

MATERIALS AND METHODS

Patients

This study was conducted in accordance with the Declaration of Helsinki and approved by the Ethical Committee of the Istituto Dermopatico dell'Immacolata (identification number 4/CE/ 2015). Written informed consent was obtained from all patients. Diagnosis of SS was based on described criteria (Olsen et al., 2007). Fresh or cryopreserved PBMCs from 25 patients with SS showing a TCR-Vβ clonality ranging from 25 to 98% (Table 1) and from a total of 14 aged-matched HDs were obtained by Ficoll-Histopaque density gradient (Sigma-Aldrich, ST. Louis, MO) and used for FC analyses. For functional analyses (ATP degradation assay, qRT-PCR, and ELISA for IL-2), CD4+ neoplastic lymphocytes were not purified if derived from samples with TCR-Vβ clonality ≥90%; otherwise, they were selected using the CD4+ untouched separation protocol (Miltenyi Biotech, Bergisch Gladbach, Germany). Therefore in these functional analyses, neoplastic cells were referred to as SS cells (Supplementary Table S2).

FC staining and analysis

Stained PBMCs were analyzed by 13- and 4-color FC on Cytoflex analyzer (Beckman Coulter, Fullerton, CA) and FACSAria cell sorter (Beckton Dickinson, Franklin Lakes, NJ).

SS cells were recognized by the expression of CD3 and CD4 in association with the specific TCR-Vβ rearrangement expression (Gibson et al., 2016) as shown in Figures 2 and 4 and Supplementary Figures S2 and S7. Alternatively, SS cells were detected by their CD3+CD4+CD49d−CD26−CD7− expression pattern (Scala et al., 2002; Scarisbrick et al., 2018) as shown in Figure 5 and Supplementary Figure S5. Blood clonality was routinely measured by IO Test beta mark TCR Vβ repertoire kit (Beckman Coulter, Fullerton, CA) (Scala et al., 2010). Further details for clonality assessment are provided in Supplementary Materials and Methods.

To track cell division during polyclonal stimulation, cells were stained with 5 μM CellTrace Violet (Thermo Fisher Scientific, Waltham, MA). Gating and frequency calculations were done with FlowJo software (Tree Star, Ashland, OR). A list of reagents used for flow cytometric analyses is reported in Supplementary Table S3.

Dimensionality reduction of FC data by Uniform Manifold Approximation and Projection analysis

Uniform Manifold Approximation and Projection (Becht et al., 2019), a nonlinear dimensionality-reduction algorithm implemented in FlowJo v10.8 Software (BD Life Sciences, Beckton Dickinson, ranklin Lakes, NJ), was used according to default settings to derive a two-dimensional plot from the multidimensional phenotypic space. The detailed method is described in Supplementary Materials and Methods.

All other procedures are described in Supplementary Materials and Methods.

Ethics statement

The study was conducted in accordance with the Declaration of Helsinki and approved by the Ethical Committee of the Istituto Dermopatico dell'Immacolata-Istituto di Ricovero e Cura a Carattere Scientifico (identification number 4/CE/2015). Informed consent was obtained from the patients.

Data availability statement

Polychromatic flow cytometry data will be provided on request from the corresponding author. The datasets of 10K and SNP6 arrays (GSE17595) are available in Gene Expression Omnibus public data repository at the following link:https://www.ncbi.nlm.nih.gov/geo/query/acc.cgi?acc=GSE17595.

ORCIDs

Mario Picozza: http://orcid.org/0000-0002-2529-6456
Cristina Cristofoletti: http://orcid.org/0000-0003-3886-2485
Antonella Bresin: http://orcid.org/0000-0003-3954-5481
Martina Fioretti: http://orcid.org/0000-0002-6606-706X
Manolo Sambucci: http://orcid.org/0000-0003-1124-7327
Enrico Scala: http://orcid.org/0000-0002-9391-9168
Alessandro Monopoli: http://orcid.org/0000-0002-9509-1405
Maria Cantonetti: http://orcid.org/0000-0003-4586-0920
Maria Antonietta Pilla: http://orcid.org/0000-0001-8757-3669
Maria Pina Accetturi: http://orcid.org/0000-0003-1682-8286
Giovanna Borsellino: http://orcid.org/0000-0002-4227-6481
Stefania D'Atri: http://orcid.org/0000-0001-9852-7377
Elisabetta Caprini: http://orcid.org/0000-0002-9732-4700
Giandomenico Russo: http://orcid.org/0000-0002-7718-9687
Maria Grazia Narducci: http://orcid.org/0000-0002-8877-4611

CONFLICT OF INTEREST

The authors state no conflict of interest.

ACKNOWLEDGMENTS

We sincerely thank the patients who contributed to this study and Rachela Simeoli for nursing assistance. The authors also thank Mauro Helmer Citterich for his technical assistance. This study was supported by The AIRC Foundation for Cancer Research in Italy (AIRC IG 17048_2015 to MGN); Italian Ministry of Healthy; and Associazione Volontari per il Policlinico Tor Vergata, ONLUS.

AUTHOR CONTRIBUTIONS

Conceptualization: MP, MGN; Formal Analysis: MP, CC, AB, MGN; Funding Acquisition: MGN; Investigation: MP, CC, AB, MF, MS; Methodology: MP, CC, EC; Project Administration: MGN; Resources: ES, AM, MC, MAP, MPA;

Supervision: MGN; Validation: MF; Writing - Original Draft Preparation: MGN, MP; Writing - Review and Editing: GB, SD, EC, GR

SUPPLEMENTARY MATERIAL

Supplementary material is linked to the online version of the paper at www.jidonline.org, and at https://doi.org/10.1016/j.jid.2022.04.017.

REFERENCES

Bagot M, Porcu P, Marie-Cardine A, Battistella M, William BM, Vermeer M, et al. IPH4102, a first-in-class anti-KIR3DL2 monoclonal antibody, in patients with relapsed or refractory cutaneous T-cell lymphoma: an international, first-in-human, open-label, phase 1 trial. Lancet Oncol 2019;20:1160–70.

Becht E, McInnes L, Healy J, Dutertre CA, Kwok IWH, Ng LG, et al. Dimensionality reduction for visualizing single-cell data using UMAP. Nat Biotechnol 2019;37:38–44.

Bensussan A, Janela B, Thonnart N, Bagot M, Musette P, Ginhoux F, et al. Identification of CD39 as a marker for the circulating malignant T-cell clone of Sézary syndrome patients. J Invest Dermatol 2019;139:725–8.

Borsellino G, Kleinewietfeld M, Di Mitri D, Sternjak A, Diamantini A, Giometto R, et al. Expression of ectonucleotidase CD39 by Foxp3+ Treg cells: hydrolysis of extracellular ATP and immune suppression. Blood 2007;110:1225–32.

Cai XY, Wang XF, Li J, Dong JN, Liu JQ, Li NP, et al. High expression of CD39 in gastric cancer reduces patient outcome following radical resection. Oncol Lett 2016;12:4080–6.

Cortés A, Gracia E, Moreno E, Mallol J, Lluís C, Canela EI, et al. Moonlighting adenosine deaminase: a target protein for drug development. Med Res Rev 2015;35:85–125.

Cristofoletti C, Bresin A, Picozza M, Picchio MC, Monzo F, Helmer Citterich M, et al. Blood and skin-derived Sezary cells: differences in proliferation-index, activation of PI3K/AKT/mTORC1 pathway and its prognostic relevance. Leukemia 2019;33:1231–42.

Cristofoletti C, Picchio MC, Lazzeri C, Tocco V, Pagani E, Bresin A, et al. Comprehensive analysis of PTEN status in Sezary syndrome. Blood 2013;122:3511–20.

Deaglio S, Dwyer KM, Gao W, Friedman D, Usheva A, Erat A, et al. Adenosine generation catalyzed by CD39 and CD73 expressed on regulatory T cells mediates immune suppression. J Exp Med 2007;204:1257–65.

Döbbeling U, Dummer R, Laine E, Potoczna N, Qin JZ, Burg G. Interleukin-15 is an autocrine/paracrine viability factor for cutaneous T-cell lymphoma cells. Blood 1998;92:252–8.

Fang F, Yu M, Cavanagh MM, Hutter Saunders J, Qi Q, Ye Z, et al. Expression of CD39 on activated T cells impairs their survival in older individuals. Cell Rep 2016;14:1218–31.

Foss FM, Koc Y, Stetler-Stevenson MA, Nguyen DT, O'Brien MC, Turner R, et al. Costimulation of cutaneous T-cell lymphoma cells by interleukin-7 and interleukin-2: potential autocrine or paracrine effectors in the Sezary syndrome. J Clin Oncol 1994;12:326–35.

Friedman DJ, Künzli BM, A-Rahim YI, Sevigny J, Berberat PO, Enjyoji K, et al. From the cover: CD39 deletion exacerbates experimental murine colitis and human polymorphisms increase susceptibility to inflammatory bowel disease. Proc Natl Acad Sci USA 2009;106:16788–93.

Gallerano D, Ciminati S, Grimaldi A, Piconese S, Cammarata I, Focaccetti C, et al. Genetically driven CD39 expression shapes human tumor-infiltrating CD8+ T-cell functions. Int J Cancer 2020;147:2597–610.

Gao C, McCormack C, van der Weyden C, Goh MS, Campbell BA, Twigger R, et al. Prolonged survival with the early use of a novel extracorporeal photopheresis regimen in patients with Sézary syndrome. Blood 2019;134:1346–50.

Gibson HM, Mishra A, Chan DV, Hake TS, Porcu P, Wong HK. Impaired proteasome function activates GATA3 in T cells and upregulates CTLA-4: relevance for Sézary syndrome. J Invest Dermatol 2013;133:249–57.

Gibson JF, Huang J, Liu KJ, Carlson KR, Foss F, Choi J, et al. Cutaneous T-cell lymphoma (CTCL): current practices in blood assessment and the utility of T-cell receptor (TCR)-Vβ chain restriction. J Am Acad Dermatol 2016;74:870–7.

Herrera A, Cheng A, Mimitou EP, Seffens A, George D, Bar-Natan M, et al. Multimodal single-cell analysis of cutaneous T-cell lymphoma reveals distinct subclonal tissue-dependent signatures. Blood 2021;138:1456–64.

Khodadoust MS, Rook AH, Porcu P, Foss F, Moskowitz AJ, Shustov A, et al. Pembrolizumab in relapsed and refractory mycosis fungoides and Sézary syndrome: a multicenter phase II study. J Clin Oncol 2020;38:20–8.

Krejsgaard T, Lindahl LM, Mongan NP, Wasik MA, Litvinov IV, Iversen L, et al. Malignant inflammation in cutaneous T-cell lymphoma-a hostile takeover. Semin Immunopathol 2017;39:269–82.

Li XY, Moesta AK, Xiao C, Nakamura K, Casey M, Zhang H, et al. Targeting CD39 in cancer reveals an extracellular ATP- and inflammasome-driven tumor immunity. Cancer Discov 2019;9:1754–73.

Ling YL, Huang X, Mitri G, Lovelace B, Pham A, Knobler R, et al. Real-world use of extracorporeal photopheresis for patients with cutaneous T-cell lymphoma in the United States: 2010–2015. J Dermatolog Treat 2020;31:91–8.

Mandapathil M, Boduc M, Roessler M, Güldner C, Walliczek-Dworschak U, Mandic R. Ectonucleotidase CD39 expression in regional metastases in head and neck cancer. Acta Otolaryngol 2018;138:428–32.

Marzec M, Liu X, Kasprzycka M, Witkiewicz A, Raghunath PN, El-Salem M, et al. IL-2- and IL-15-induced activation of the rapamycin-sensitive mTORC1 pathway in malignant CD4+ T lymphocytes. Blood 2008;111:2181–9.

Melchiotti R, Puan KJ, Andiappan AK, Poh TY, Starke M, Zhuang L, et al. Genetic analysis of an allergic rhinitis cohort reveals an intercellular epistasis between FAM134B and CD39. BMC Med Genet 2014;15:73.

Mirza AS, Horna P, Teer JK, Song J, Akabari R, Hussaini M, et al. New insights into the complex mutational landscape of Sézary syndrome. Front Oncol 2020;10:514.

Moesta AK, Li XY, Smyth MJ. Targeting CD39 in cancer. Nat Rev Immunol 2020;20:739–55.

Nagate Y, Ezoe S, Fujita J, Okuzaki D, Motooka D, Ishibashi T, et al. Ectonucleotidase CD39 is highly expressed on ATLL cells and is responsible for their immunosuppressive function. Leukemia 2021;35:107–18.

Narducci MG, Scala E, Bresin A, Caprini E, Picchio MC, Remotti D, et al. Skin homing of Sézary cells involves SDF-1-CXCR4 signaling and down-regulation of CD26/dipeptidylpeptidase IV. Blood 2006;107:1108–15.

Narducci MG, Tosi A, Frezzolini A, Scala E, Passarelli F, Bonmassar L, et al. Reduction of T lymphoma cells and immunological invigoration in a patient concurrently affected by melanoma and Sezary syndrome treated with nivolumab. Front Immunol 2020;11:1–16.

Olsen E, Vonderheid E, Pimpinelli N, Willemze R, Kim Y, Knobler R, et al. Revisions to the staging and classification of mycosis fungoides and Sezary syndrome: a proposal of the International Society for cutaneous Lymphomas (ISCL) and the cutaneous lymphoma task force of the European Organization of Research and Treatment of Cancer (EORTC). Blood 2007;110:1713–22.

Olsen EA, Whittaker S, Kim YH, Duvic M, Prince HM, Lessin SR, et al. Clinical end points and response criteria in mycosis fungoides and Sézary syndrome: a consensus statement of the International Society for cutaneous Lymphomas, the United States Cutaneous Lymphoma Consortium, and the Cutaneous Lymphoma Task Force of the European Organisation for Research and Treatment of Cancer. J Clin Oncol 2011;29:2598–607.

Park J, Daniels J, Wartewig T, Ringbloom KG, Martinez-Escala ME, Choi S, et al. Integrated genomic analyses of cutaneous T-cell lymphomas reveal the molecular bases for disease heterogeneity. Blood 2021;138:1225–36.

Perrot I, Michaud HA, Giraudon-Paoli M, Augier S, Docquier A, Gros L, et al. Blocking antibodies targeting the CD39/CD73 immunosuppressive pathway unleash immune responses in combination cancer therapies. Cell Rep 2019;27:2411–25.e9.

Poszepczynska-Guigné E, Schiavon V, D'Incan M, Echchakir H, Musette P, Ortonne N, et al. CD158k/KIR3DL2 is a new phenotypic marker of Sezary cells: relevance for the diagnosis and follow-up of sezary syndrome. J Invest Dermatol 2004;122:820–3.

Pulte D, Furman RR, Broekman MJ, Drosopoulos JHF, Ballard HS, Olson KE, et al. CD39 expression on T lymphocytes correlates with severity of disease in patients with chronic lymphocytic leukemia. Clin Lymphoma Myeloma Leuk 2011;11:367–72.

Qi Y, Xia Y, Lin Z, Qu Y, Qi Y, Chen Y, et al. Tumor-infiltrating CD39+CD8+ T cells determine poor prognosis and immune evasion in clear cell renal cell carcinoma patients. Cancer Immunol Immunother 2020;69:1565–76.

Rassek K, Iżykowska K. Single-cell heterogeneity of cutaneous T-cell lymphomas revealed using RNA-seq technologies 2020;12:1–15.

Rissiek A, Baumann I, Cuapio A, Mautner A, Kolster M, Arck PC, et al. The expression of CD39 on regulatory T cells is genetically driven and further upregulated at sites of inflammation. J Autoimmun 2015;58:12–20.

Samimi S, Benoit B, Evans K, Wherry EJ, Showe L, Wysocka M, et al. Increased programmed death-1 expression on CD4+ T cells in cutaneous T-cell lymphoma: implications for immune suppression. Arch Dermatol 2010;146:1382–8.

Scala E, Abeni D, Pomponi D, Narducci MG, Lombardo GA, Mari A, et al. The role of 9-O-acetylated ganglioside D3 (CD60) and {alpha}4{beta}1 (CD49d) expression in predicting the survival of patients with Sézary syndrome. Haematologica 2010;95:1905–12.

Scala E, Narducci MG, Amerio P, Baliva G, Simoni R, Giovannetti A, et al. T cell receptor-Vα analysis identifies a dominant $CD60^{+}CD26^{-}CD49d^{-}$T cell clone in the peripheral blood of Sézary syndrome patients. J Invest Dermatol 2002;119:193–6.

Scarisbrick JJ, Hodak E, Bagot M, Stranzenbach R, Stadler R, Ortiz-Romero PL, et al. Blood classification and blood response criteria in mycosis fungoides and Sézary syndrome using flow cytometry: recommendations from the EORTC cutaneous lymphoma task force. Eur J Cancer 2018;93:47–56.

Scarisbrick JJ, Prince HM, Vermeer MH, Quaglino P, Horwitz S, Porcu P, et al. Cutaneous lymphoma international consortium study of outcome in advanced stages of mycosis fungoides and Sézary syndrome: effect of specific prognostic markers on survival and development of a prognostic model. J Clin Oncol 2015;33:3766–73.

Shalabi D, Bistline A, Alpdogan O, Kartan S, Mishra A, Porcu P, et al. Immune evasion and current immunotherapy strategies in mycosis fungoides (MF) and Sézary syndrome (SS). Chin Clin Oncol 2019;8:11.

Sonigo G, Bozonnat A, Dumont M, Thonnart N, Ram-Wolff C, de Masson A, et al. Involvement of the CD39/CD73/adenosine pathway in T-cell proliferation and NK cell-mediated antibody-dependent cell cytotoxicity in Sézary syndrome. Blood 2022;139:2712–6.

Spolski R, Li P, Leonard WJ. Biology and regulation of IL-2: from molecular mechanisms to human therapy. Nat Rev Immunol 2018;18:648–59.

Wall MJ, Wigmore G, Lopatář J, Frenguelli BG, Dale N. The novel NTPDase inhibitor sodium polyoxotungstate (POM-1) inhibits ATP breakdown but also blocks central synaptic transmission, an action independent of NTPDase inhibition. Neuropharmacology 2008;55:1251–8.

Wilcox RA. Cutaneous T-cell lymphoma: 2017 update on diagnosis, risk-stratification, and management. Am J Hematol 2017;92:1085–102.

Willemze R, Jaffe ES, Burg G, Cerroni L, Berti E, Swerdlow SH, et al. WHO-EORTC classification for cutaneous lymphomas. Blood 2005;105:3768–85.

SUPPLEMENTARY MATERIALS AND METHODS

Assessment of Sézary syndrome cell clonality

Blood clonality was measured by IO Test beta mark TCR Vβ repertoire kit (Beckman Coulter, Fullerton, CA) covering about 70% of the normal TCR Vβ repertoire, as described (Scala et al., 2010). Sézary syndrome (SS) cells with unrecognized TCR Vβ chains (TCR Vβ null) were distinguished by simultaneous staining with CD3, CD4, and all FITC/phycoerythrin-conjugated anti−TCR-Vβ antibodies contained in the kit followed by gating on CD3+CD4 + cells not labeled for FITC and phycoerythrin signals. Alternatively, SS cell detection was performed by their CD3+CD4+CD49d−CD26−CD7− expression pattern (Scala et al., 2002)

Dimensionality reduction of flow cytometry data by Uniform Manifold Approximation and Projection analysis

Uniform Manifold Approximation and Projection (Becht et al., 2019), a nonlinear dimensionality-reduction algorithm implemented in FlowJo, was used according to default settings to derive a two-dimensional plot from the multidimensional phenotypic space. An equal number of events (5,826) randomly sampled from live CD4+ T cells from each of the nine data files were electronically barcoded to recognize sample number (coded as identification number) and healthy (red) or pathological (blue) status and concatenated into a single file for simultaneous analysis by this machine-learning technique. Data were then analyzed by Uniform Manifold Approximation and Projection, which convert the information deriving from the CD4+ cell−tailored phenotypic features (i.e., CD49d, CD39, CD158k, PD-1, CD127, CD25, CD62L, and CCR7) (Fig.1a left) into two dimensions.

Genotyping

For genetic studies, SS cell isolation and genomic DNA extraction were performed as previously described (Caprini et al., 2009). The SNP in the *ENTPD1* gene (rs10748643 A>G) was PCR amplified using the primers pair and conditions as described (Rissiek et al., 2015). PCR products were sequenced using the Sanger method with either forward or reverse primer.

Adenosine triphosphate degradation assay

The assay was performed by incubating 2.5×10^5 SS cells obtained from G/G (n = 3) and A/A (n = 3) patients (Supplementary Table S1) with 1 μM adenosine triphosphate (Sigma-Aldrich, St. Lious, MO). The concentration of adenosine triphosphate was determined at different time points in culture supernatants using a luciferase-based assay (Cell Titer-GLO by Promega, Madison, WI) read by Ensight Instrument (PerkinElmer, Waltham, MA). When indicated, the cells were preincubated for 30 minutes at 37 °C with 250 μM of the CD39 inhibitor ARL67156 (Santa Cruz Biotechnology, Dallas, TX) or 100 μM POM-1.

Analysis of CD39 expression on cell stimulation

Fresh PBMCs from patients with SS carrying the G/G (n = 3) or the A/A (n = 3) genotype were cultured in 48-well plates at the concentration of 1×10^6 cells per well in 1 ml of RPMI 1640 medium (Euroclone, Pero [MI], Italy) supplemented with 10% fetal bovine serum without or with Dynabeads Human T-Activator CD3/CD28 beads (Thermo Fisher Scientific, Waltham, MA) at a ratio of 1:1 (bead:cells). After 4 days, the beads were removed, and half of the cells were harvested, washed, stained with antibodies against surface markers, and analyzed by flow cytometry. The same analyses were performed for the remaining cells left in culture for additional 6 days in a complete medium without stimuli.

Viability of follow-up (F-up) SS samples derived from two of six patients analyzed as described earlier (SS96 F-up, TCR Vβ13.1 and SS98 F-up, TCR Vβ8) plus a new one (SS111, TCR Vβ13.1) was determined by flow cytometry in a set of experiments independent from those addressing the CD39 expression on stimulation. Apoptotic SS cells were recognized by CD3/CD4/specific TCR-Vβ staining in combination with Annexin-V on day 0, day 4 after stimulation by anti-CD3/CD28 beads, and 6 days after beads removal (day 10) as shown in Supplementary Figure S7. Clonality calculated as the percentage of SS cells within total CD3+CD4+ T-cells at each time point was also shown

Effects of CD39 inhibition on cell activation/proliferation and apoptosis and IL-2 production

PBMCs obtained from G/G and A/A patients were stimulated for 4 days with beads used at a 1:2 ratio with or without POM-1 (Tocris, catalog number 2689, Biotechne, Bristol, United Kingdom) used at 10 μM. In all experiments, POM-1 was added to the medium each day to avoid serum half-life.

Before the intracellular IL-2 detection, cells were restimulated on day 4 with phorbol myristate acetate and ionomycin used at 0.02 and 0.2 μg/ml, respectively (Sigma-Aldrich) in the presence of Brefeldin A (10 μg/μl, Sigma-Aldrich) for the last 5 hours. The clinical characteristics of patients employed for these analyses are summarized in Supplementary Table S2.

Viability and proliferation of stimulated SS cells evaluated by MTT assay and cell count

Viability and proliferation of F-up SS samples derived from three of six patients analyzed earlier (SS96 F-up, SS98 F-up, and SS112 F-up) plus a new one (SS111) were also determined by MTT assay (3-(4,5-di**methylthiazol**-2-yl)-2,5-diphenyl**tetrazolium** bromide) and cell count, respectively. SS cells were purified using the CD4+ untouched separation protocol (Miltenyi Biotech, Bergisch Gladbach, Germany) and analyzed at day 0 and after 4 days of stimulation with anti-CD3/CD28 beads used at a 1:2 ratio without cytokine support. MTT assay was performed as previously described (Cristofoletti et al., 2019), whereas detached cells from beads were counted by hemocytometer and trypan blue staining. The results are shown in Supplementary Figure S8.

Analysis of apoptosis in CD39^{high} and CD39^{low} SS cells derived from patient SS88

PBMCs obtained from patient SS88 were stimulated for 6 days with anti-CD3/CD28 beads used at a ratio of 1:5. Apoptosis was also evaluated in PBMCs cultured for 6 days at basal condition using RPMI 1640 medium supplemented with 10% fetal bovine serum. Early apoptotic SS cells were detected as Annexin-V+Live/Dead−, late apoptotic SS cells were detected as annexinV+ live/dead+, and primary necrotic SS cells were detected as annexinV−live/dead+.

IL-2 measurement by qRT-PCR and ELISA

Total RNA was extracted and used for cDNA synthesis as described (Cristofoletti et al., 2013). TaqMan Gene expression assay (Applied Biosystems, Waltham, MA) was conducted on SS cells derived from G/G and A/A patients unstimulated (day 0) or activated for 4 days (day 4) with anti-CD3/CD28 beads used at 1:2 ratio. Relative expression of IL-2 (Hs00174114_m1, Thermo Fisher Scientific) and IL-2 receptor (Hs00907777_m1) was calculated using the comparative Ct method ($2^{-\Delta\Delta Ct}$) and actin-β (Hs00357333_g1) as internal reference gene (Livak and Schmittgen, 2001). The expression of *IL2* mRNA relative to actin-β mRNA of each sample was determined using the formula $2^{-\Delta Ct} \times 10^4$ where $\Delta Ct = (Ct_{IL\text{-}2} - Ct_{actin\text{-}\beta})$ (Livak and Schmittgen, 2001). Cell supernatants from 2×10^6 SS cells derived from G/G (n = 5) and A/A (n = 6) patients cultured in 1 ml of complete medium with anti-CD3/CD28 beads used at a ratio of 1:2 were collected after 4 days and measured for IL-2 by ELISA assay (Thermo Fisher Scientific). A total of 450–550 absorbance was measured using Ensight (PerkinElmer, Waltham, MA).

Survival and statistical analysis

Statistical analyses and graphs were carried out with the software Graphpad PRISM (by GraphPad Software, La Jolla, CA). Survival was evaluated by Kaplan–Meier estimator. $P \leq 0.05$ was considered significant.

SUPPLEMENTARY REFERENCES

Becht E, McInnes L, Healy J, Dutertre CA, Kwok IWH, Ng LG, et al. Dimensionality reduction for visualizing single-cell data using UMAP. Nat Biotechnol 2019;37:38–44.

Caprini E, Cristofoletti C, Arcelli D, Fadda P, Citterich MH, Sampogna F, et al. Identification of key regions and genes important in the pathogenesis of Sézary syndrome by combining genomic and expression microarrays. Cancer Res 2009;69:8438–46.

Cristofoletti C, Bresin A, Picozza M, Picchio MC, Monzo F, Helmer Citterich M, et al. Blood and skin-derived Sezary cells: differences in proliferation-index, activation of PI3K/AKT/mTORC1 pathway and its prognostic relevance. Leukemia 2019;33:1231–42.

Cristofoletti C, Picchio MC, Lazzeri C, Tocco V, Pagani E, Bresin A, et al. Comprehensive analysis of PTEN status in Sezary syndrome. Blood 2013;122:3511–20.

Livak KJ, Schmittgen TD. Analysis of relative gene expression data using real-time quantitative PCR and the 2(-delta delta C[T]) method. Methods 2001;25:402–8.

Rissiek A, Baumann I, Cuapio A, Mautner A, Kolster M, Arck PC, et al. The expression of CD39 on regulatory T cells is genetically driven and further upregulated at sites of inflammation. J Autoimmun 2015;58:12–20.

Scala E, Abeni D, Pomponi D, Narducci MG, Lombardo GA, Mari A, et al. The role of 9-O-acetylated ganglioside D3 (CD60) and {alpha}4{beta}1 (CD49d) expression in predicting the survival of patients with Sézary syndrome. Haematologica 2010;95:1905–12.

Scala E, Narducci MG, Amerio P, Baliva G, Simoni R, Giovannetti A, et al. T cell receptor-Vα analysis identifies a dominant $CD60^+CD26^-CD49d^-$T cell clone in the peripheral blood of Sézary syndrome patients. J Invest Dermatol 2002;119:193–6.

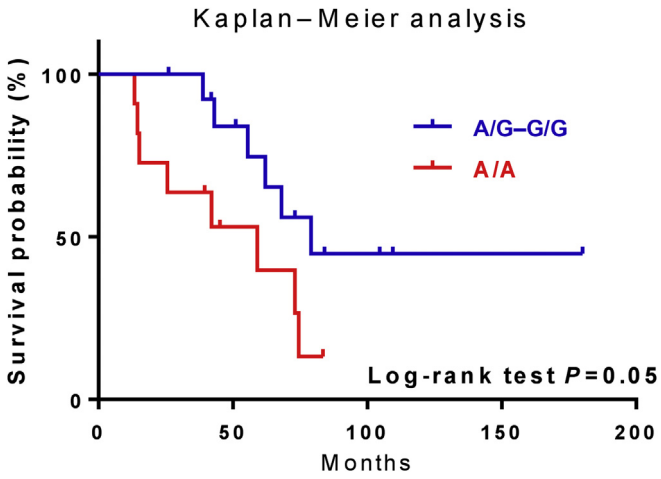

Supplementary Figure S1. SNP rs10748643 genotype correlates with the outcome of patients with SS regardless of *PTEN* genetic status. Comparison of survival between patients with SS with A/A and A/G–G/G SNP without chromosome 10q32 loss (n = 25, $P = 0.05$). Statistics were calculated by the log-rank test. SS, Sézary syndrome.

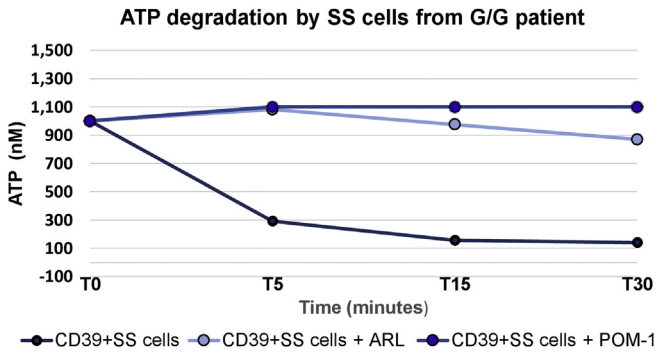

Supplementary Figure S3. CD39 enzymatic activity of CD39+ SS cells is blocked by both ARL67156 and POM-1. SS cells derived from patient SS96 carrying a G/G genotype were evaluated for their ability to degrade 1 μM of ATP at different times in the absence or presence of CD39 inhibitors ARL67156 and POM-1. After 30 minutes, POM-1 appeared more effective than ARL67156. ATP, adenosine triphosphate; SS, Sézary syndrome.

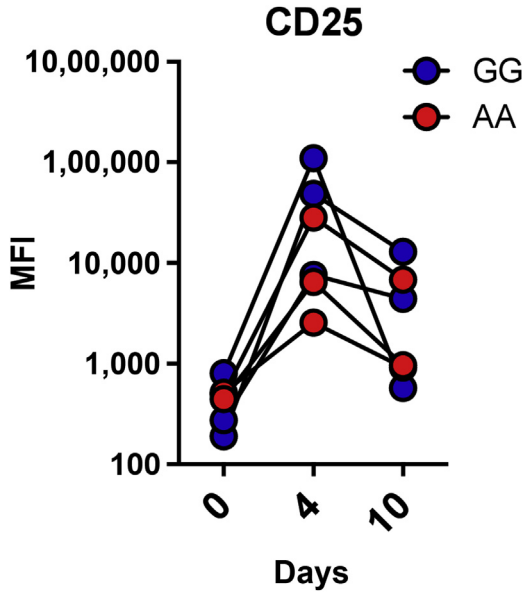

Supplementary Figure S2. IL-2 receptor (CD25) upregulation by SS cell after activation. PBMCs from patients with an A/A SNP genotype (n = 3, in red) and with G/G SNP genotype (n = 3, in blue) were stimulated with anti-CD3/CD28 beads at a 1:1 ratio in a complete medium. Flow cytometric analysis of CD25 expression was done on day 0 (baseline), on day 4 after stimulation, and 6 days after bead removal (day 10). Changes in the MFI for CD25 expression were measured in A/A samples (in red) and G/G samples (in blue). MFI, median of fluorescent intensity; SS, Sézary syndrome.

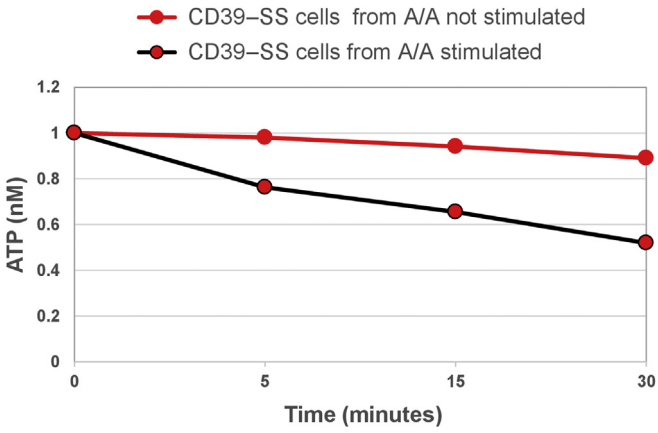

Supplementary Figure S4. CD39 enzymatic activity of CD39^{low} SS cells is enhanced during stimulation. SS cells derived from patient SS105 carrying the A/A genotype were cultured in a complete medium for 4 days without or with anti-CD3/CD28 beads used at a 1:1 ratio and then evaluated for their ability to degrade 1 μM ATP at different times. ATP, adenosine triphosphate; SS, Sézary syndrome.

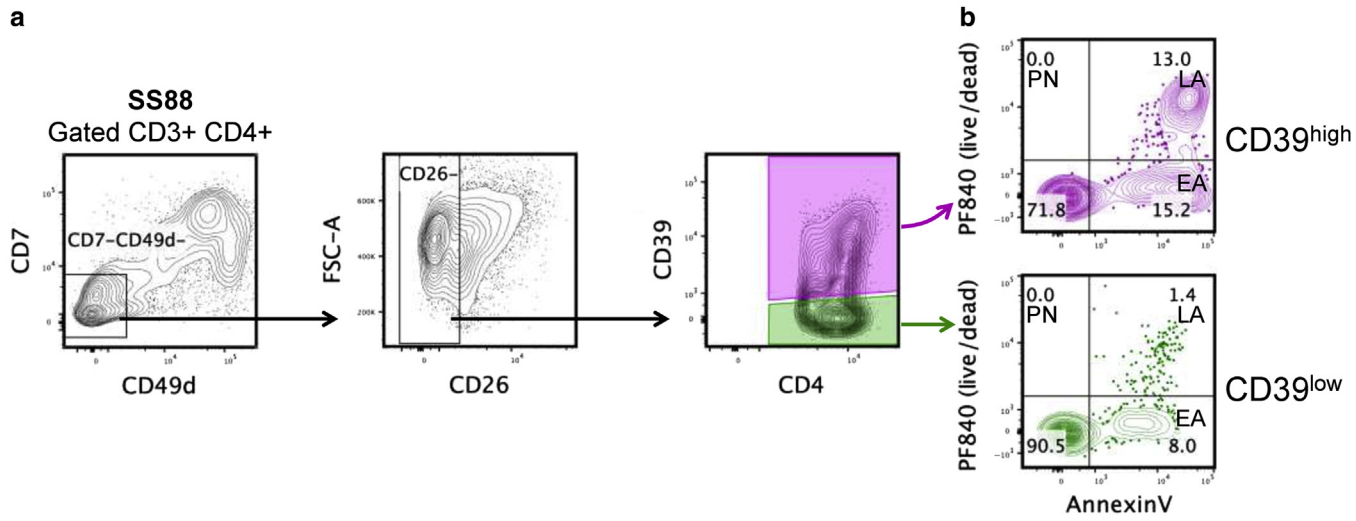

Supplementary Figure S5. CD39^{high} SS cells show higher apoptosis than CD39^{low} SS cells. PBMCs from patient SS88 on T3 were cultured for 6 days in a complete medium without stimulation. **(a)** CD7−CD49d−CD26− cells were electronically separated from CD3+ CD4+ lymphocytes by sequential gating. The resulting enriched SS cells were fractionated into two subsets on the basis of CD39 expression, and each subset was visualized on 2D contour plots to measure percentages of **(b)** EA (annexinV+ live/dead−), LA (annexinV+ live/dead+), and PN (annexinV− live/dead+) cells. 2D, two dimensional; EA, early apoptotic; FSC-A, forward scatter area; LA, late apoptotic; PN, primary necrotic; SS, Sézary syndrome; T4, day 4.

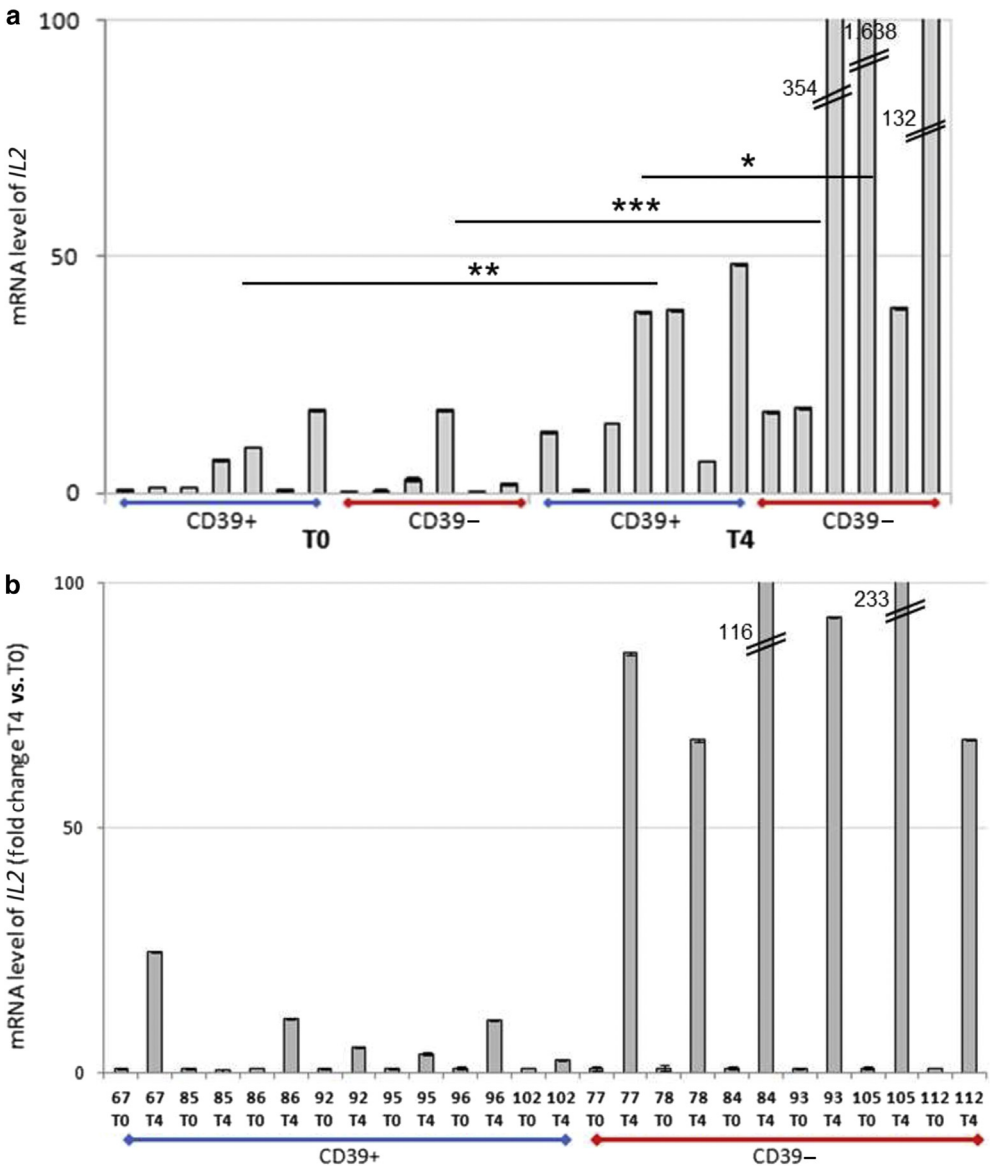

Supplementary Figure S6. mRNA level of *IL2* measured by qRT-PCR. mRNA levels of *IL2* were measured in CD39+ SS cells derived from G/G (blue) and in CD39− SS cells from A/A (red) patients at baseline (T0) and after 4 days (T4) of stimulation with anti-CD3/CD28 beads. **(a)** Data are expressed as mRNA levels calculated using β-actin as an endogenous reference control for normalization by the $2^{\wedge -\Delta Ct} \times 10^4$ formula, where $\Delta Ct = (Ct_{IL\text{-}2} - Ct_{actin\text{-}\beta})$. $^{***}P = 0.0001$ and $^{**}P = 0.01$ with paired ratio two-tailed *t*-test and $^{*}P = 0.05$ for with unpaired two-tailed *t*-test **(b)** Data are expressed as T4 mRNA fold change calculated versus T0 by $2^{\wedge -\Delta\Delta Ct}$ formula, where $\Delta\Delta Ct = (Ct_{IL\text{-}2} - Ct_{actin\text{-}\beta})_{T4} - (Ct_{IL\text{-}2} - Ct_{actin\text{-}\beta})_{T0}$. $P = 0.0012$ with unpaired two-tailed *t*-test. SS, Sézary syndrome; T0, day 0; T4, day 4.

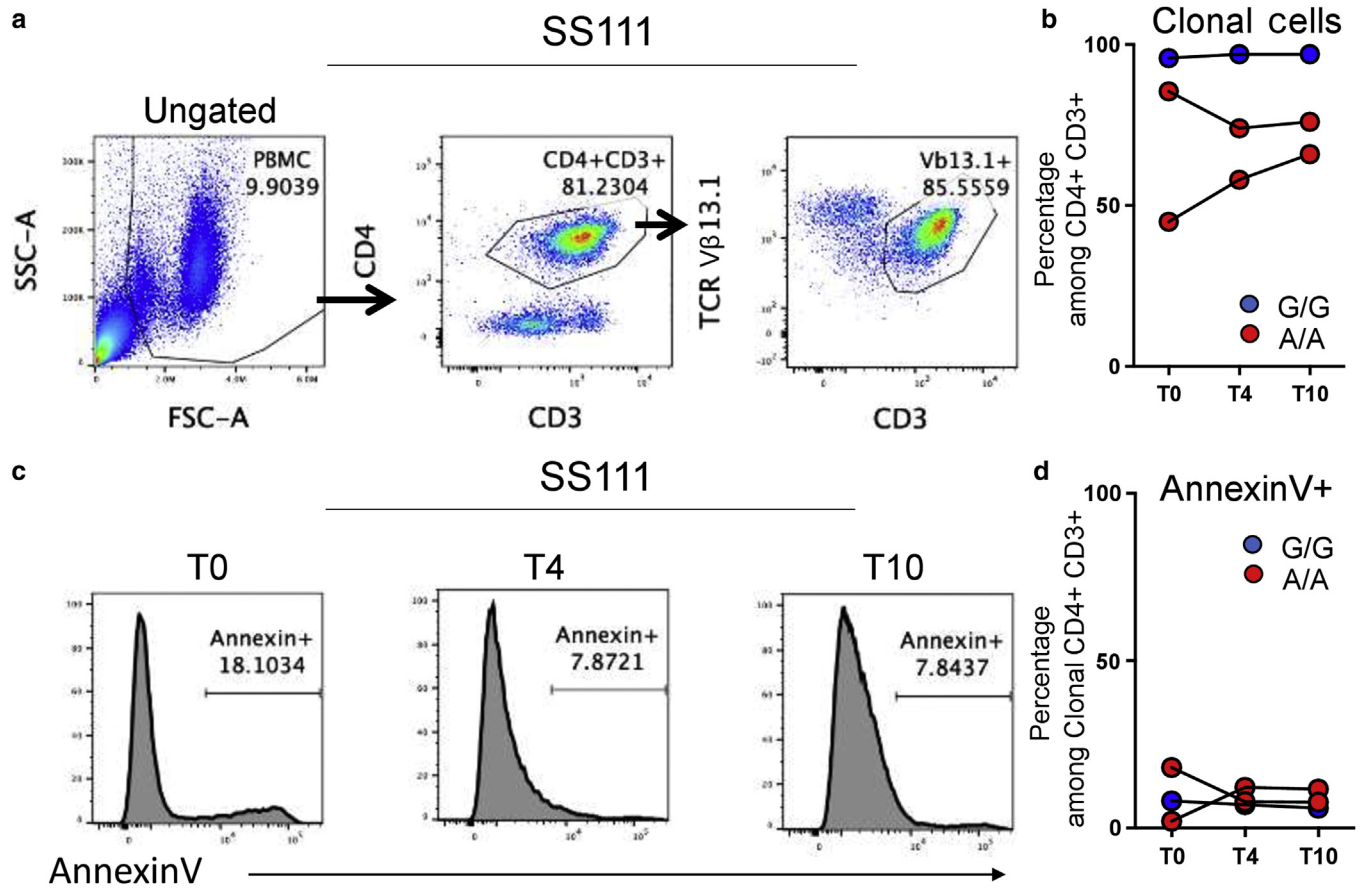

Supplementary Figure S7. Apoptotic rates of SS cells evaluated after 4 days of anti-CD3/CD28 beads stimulation and 6 days after removing the beads. PBMCs from one G/G (SS96 F-up, TCR Vβ13.1, in blue) and two A/A patients (SS98 F-up, TCR Vβ8 and SS111, TCR Vβ13.1, in red) were analyzed by FC on day 0, day 4 after anti-CD3/CD28 stimulation, and 6 days after beads removal (day 10). At each time point, the analysis of clonality by specific anti−TCR Vβ-chain antibodies and of apoptosis by annexin-V staining was conducted. **(a)** Gating strategy to identify the clonal cells in a representative patient with SS. **(b)** Cumulative clonality values (i.e., TCR Vβ+ cell frequencies). **(c)** Histogram plots showing annexin-V staining of clonal cells from one representative patient with SS. **(d)** Compiled results of annexin-V staining. Differences found were not significant by paired two-tailed *t*-test. FC, flow cytometry; FSC-A, forward scatter area; F-up, follow-up; SS, Sézary syndrome; SSC-A, side scatter area.

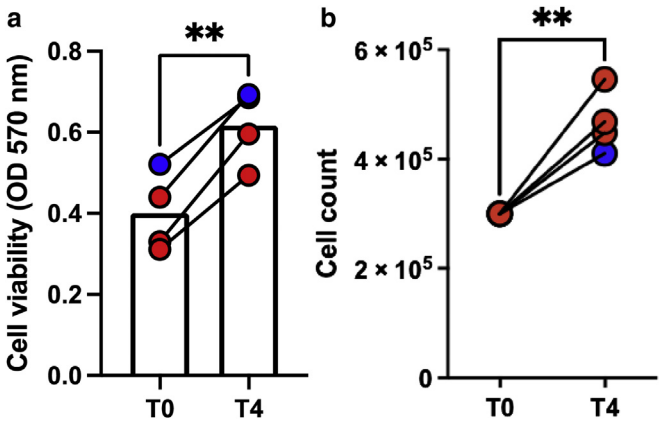

Supplementary Figure S8. Viability and proliferation of SS cells stimulated for 4 days with anti-CD3/CD28 beads without cytokine support were evaluated by MTT assay and cell count. SS cells purified from the blood of four patients with SS (SS96 F-up, SS98 F-up, SS111 F-up, and SS112) were plated in flat 96-well plates at 3×10^5/well and measured at T0 and after 4 days (T4) of stimulation with anti-CD3/CD28 beads used at 1:2 ratio. **(a)** Cell viability was evaluated by MTT assay (M2128, Sigma-Aldrich, St. Louis, MO). Data are expressed as means of optical densities ± SD measured at 570 nm by an Ensight microplate reader (PerkinElmer, Waltham, MA). **(b)** Detached cells from beads were counted by hemocytometer and trypan blue staining. Statistics were calculated by paired *t*-test. $^{**}P \leq 0.009$. F-up, follow-up; OD, optical density; SS, Sézary syndrome; T0, day 0; T4, day 4.

Supplementary Table S1. SS Patients Analyzed for SNP rs10748643 Genotype, CD39 Expression, and Survival Analysis

SS ID	Copy Number[1]	Genotype[2]	$CD39^+/CD4^+$ Cells (%)[3]	Survival (mo)	Status	KM Estimator
02	LOSS	G/–	NA	75	DD	√
08	WT	A/A	NA	73	DD	√
11	WT	A/A	NA	NA	NA	NA
15	LOSS	A/–	NA	NA	NA	NA
23	WT	G/G	NA	79	DD	√
25	WT	A/A	NA	25	DD	√
27	WT	A/G	NA	180	AD	√
28	WT	A/A	NA	15	DD	√
30	**WT**	**G/G**	**76.4**	105	AD	√
32	**LOSS**	**A/–**	**0.9**	40	DD	√
34	LOSS	A/–	NA	31	AD	√
35	WT	A/A	NA	40	AD	√
36	LOSS	G/–	NA	48	AD	√
37	WT	A/G	NA	43	DD	√
38	WT	A/G	NA	84	AD	√
39	LOSS	A/–	NA	26	DD	√
40	WT	G/G	NA	110	AD	√
41	WT	A/A	NA	59	DD	√
42	LOSS	G/–	NA	67	DD	√
43	WT	G/G	NA	39	DD	√
45	**WT**	**A/A**	**7.7**	43	DD	√
48	LOSS	G/–	NA	48	DD	√
49	WT	A/A	NA	75	DD	√
50	**WT**	**A/A**	**2.0**	99	DD	√
51	WT	A/G	NA	68	DD	√
53	LOSS	A/A	NA	21	DD	√
55	LOSS	A/–	NA	25	DD	√
57	LOSS	A/G	NA	42	AD	√
58	LOSS	G/–	NA	28	DD	√
60	**WT**	**A/G**	**65.5**	56	DD	√
61	**LOSS**	**A/–**	**4.2**	30	DD	√
62	WT	A/A	NA	13	DD	√
63	WT	A/A	NA	35	DD	√
64	**LOSS**	**A/–**	**15.4**	54	AD	√
65	WT	G/G	NA	62	DD	√
66	WT	A/A	NA	15	DD	√
67	**LOSS**	**G/–**	**67.5**	229	AD	√
68	LOSS	G/G	NA	54	DD	√
69	WT	A/G	NA	31	DD	√
70	WT	A/G	NA	51	AD	√
72	**NA**	**A/G**	**28.4**	**NA**	**NA**	**NA**
74	**NA**	**A/A**	**6.5**	**NA**	**NA**	**NA**
76	**NA**	**A/G**	**83.8**	63	DD	√
77	**NA**	**A/A**	**4.7**	92	DD	√
78	**NA**	**A/A**	**2.4**	59	DD	√
80	NA	NA	74.2	NA	NA	NA
81	**NA**	**A/G**	**86.0**	**NA**	**NA**	**NA**
82	**NA**	**G/G**	**97.0**	**NA**	**NA**	**NA**
83	**NA**	**A/A**	**1.0**	43	DD	√
84	**NA**	**A/A**	**NA**	64	AD	√
85	**NA**	**G/G**	**95.0**	57	DD	√
86	**NA**	**G/G**	**99.0**	**NA**	**NA**	**NA**
87	**NA**	**A/G**	**80.0**	57	AD	√
88	**NA**	**A/G**	**48.0**	66	AD	√
94	**NA**	**G/G**	**NA**	37	DD	√
96	**NA**	**G/G**	**97.0**	**NA**	**NA**	**NA**
98	**NA**	**A/A**	**10.0**	**NA**	**NA**	**NA**
103	**NA**	**A/A**	**10.0**	**NA**	**NA**	**NA**
105	**NA**	**A/A**	**5.0**	**NA**	**NA**	**NA**

Abbreviations: AD, alive with disease; DD, dead of disease; ID, identification; KM, Kaplan–Meier; NA, not available; SS, Sézary syndrome; WT, wild type.

Patients with SS are in bold. Data were analyzed by Sanger sequencing and flow cytometry.

[1]By 10K and SNP6 arrays

[2]By 10K and SNP6 arrays and/or Sanger sequencing

[3]By FACS.

Supplementary Table S2. Clinical Characteristics of Patients Whose SS Cells Were Used for Functional Studies

SS ID	Sex/ Age	TCR-Vβ Family	%TCR-Vβ+ within CD3+/ CD4+	CD39 Genotype	% of CD39 + SS Cells within Total CD4+	CD39 Expression on Anti-CD3/ CD28 Stimulation	ATP Degradation Assay	Activation and Proliferation during POM-1 Treatment	Apoptosis during POM-1 Treatment	Intracellular IL-2 Staining during POM-1 Treatment	qRT-PCR for IL-2 and IL-2R	ELISA for IL-2
67	66/F	2	82	G/G (1G)	70.7				√	√	√	√
85	78/F	13.6	52	G/G	94						√	√
86	54/F	Null	97	G/G	99	√	√	√	√	√	√	√
87	61/F	Null	87	G/G	80	√	√					
92	48/M	Null	78	G/G	nd						√	√
95	72/F	5.1	95	G/G	nd						√	
96	75/M	13.1	98	G/G	99	√	√	√			√	
102	74/M	7	92	G/G	nd						√	√
77	51/F	Null	74	A/A	0.9			√		√	√	√
78	82/F	Null	95	A/A	2.4			√			√	√
84	75/M	1	93	A/A	nd						√	√
93	67/M	Null	93	A/A (1A)	nd						√	√
98	56/F	8	60	A/A	10	√	√	√		√		
103	71/M	5.2	63	A/A	3	√	√					
105	66/M	5.1	95	A/A	5	√	√		√		√	√
112	65/F	Null	93	A/A	8			√	√	√	√	√

Abbreviations: ATP, adenosine triphosphate; F, female; M, male; nd, not done; SS, Sézary syndrome.

Supplementary Table S3. Reagents Used for Flow Cytometric Analyses

Fluorochrome	Specificity	Vendor	Dilution	Figure Number
APC	CD25	BD	1/30	1
APC-Alexa700	CD3	Coulter	1/100	1 and 5
APC-eFluor780	CCR7	eBiosciences	1/30	1
APC-R700	IL-2	BD	1/60	5
Aqua	Dead cells	BioLegend	1/300	1
BUV395	CD3	BD	1/30	5
BUV395	CD71	BD	1/60	5
BUV661	CD25	BD	1/60	5
BV421	PD-1	BD	1/50	1
BV605	CD26	BD	1/100	5
BV605	CD4	BD	1/100	1
BV650	CD8	BioLegend	1/30	1
BV785	CD127	BioLegend	1/30	1
FITC	CD49d	Immunotools	1/100	1, 2, and 3
FITC	CD7	BioLegend	1/60	5
IFluor810	CD4	AAT Bioquest	1/200	5
PE	CD158k	R&D	1/30	1
PE	CD39	Miltenyi	1/100	2-4
PE-CF594	CD39	BD	1/120	1
PE-CF594	CD49d	BD	1/100	5
PE-Cy5	CD49d	Coulter	1/60	5
PE-Cy5.5	CD19	Coulter	1/200	1
PE-Cy7	CD62L	BD	1/100	1
PerCP-Cy5.5	CD25	BD	1/100	5
PerCP-Cy5.5	CD4	Miltenyi	1/60	2–4
PromoFluor840	Dead cells	PromoCell	1/300	5
Violet	Amines	ThermoFisher	5 μM	5

Abbreviations: APC, allophycocyanin; PE, phycoerythrin.